Determination of Internuclear Distances and the Orientation of Functional Groups by Solid-State NMR: Rotational Resonance Study of the Conformation of Retinal in Bacteriorhodopsin†

A. E. McDermott,‡,§ F. Creuzet,‡,⊥ R. Gebhard,∥ K. van der Hoef,∥ M. H. Levitt,⊛ J. Herzfeld,▽ J. Lugtenburg,∥ and R. G. Griffin*,‡

Francis Bitter National Magnet Laboratory and Department of Chemistry, Massachusetts Institute of Technology, Cambridge, Massachusetts 02139, Gorlaeus Laboratorium, Rijksuniversiteit te Leiden, NL-2300 RA Leiden, The Netherlands, Department of Chemistry, Brandeis University, Waltham, Massachusettsin 02254, and Physical Chemistry, Arrhenius Laboratory, Stockholm University, S10691 Stockholm, Sweden

Received September 2, 1993⊛

ABSTRACT: We have used a new solid-state NMR technique—rotational resonance—to determine both internuclear distances and the relative orientations of chemical groups (dihedral angles) in retinal bound to bacteriorhodopsin (bR) and in retinoic acid model compounds. By matching the rotational resonance condition ($\delta = n\omega_r/2\pi$, where δ is the difference in isotropic chemical shifts for two dipolar coupled spins, $\omega_r/2\pi$ is the mechanical rotational frequency of the sample in the MAS experiment, and n is a small integer denoting the order of the resonance), we selectively reintroduce the dipolar coupling and enhance the rate of magnetization exchange. Spectroscopic data and theoretical simulations of the magnetization exchange trajectories for the 8,18-^{13}C dipolar coupled pair in retinoic acid model compounds, crystallized in both the 6-s-*cis* and 6-s-*trans* forms, indicate that an accurate determination of the internuclear distance is possible. For the $n = 1$ resonance we find the distance determination to be reasonably independent of the relative orientation of the groups. In contrast, for the $n = 2$ resonance, there is a more pronounced dependence on the relative orientation of the groups which permits an estimate of the angle around the 6-s bond for the *cis* and *trans* forms to be 42 ± 5° and 90 ± 10°, respectively, in good agreement with crystallography. In bR we demonstrate that the 8-^{13}C–18-^{13}C distance is 4.1 Å and the average 8-^{13}C–16-^{13}C/8-^{13}C–17-^{13}C distance is 3.3–3.5 Å. These distance determinations depend somewhat on assumed values for the relaxation processes of the zero-quantum state T_2^{ZQ}, and the resulting errors are larger than in the model compounds, but probably less than 0.4 Å. The data on bR demonstrate unambiguously that the retinal is in a 6-s-*trans* conformation, confirming the previous interpretation of ^{13}C chemical shift data and other measurements. Our work clearly suggests that dihedral angle measurements should also be possible with additional orders of rotational resonance. These studies demonstrate a new and robust method for determining internuclear distances and chemical orientations. The prospects appear very encouraging for measuring C–C distances up to 5.0 or 6.0 Å, with an accuracy of better than 0.4 Å in very large enzymes, and in some cases for determining the relative orientation of chemical groups.

We have recently introduced a new solid-state NMR method for measurement of internuclear distances in polycrystalline and amorphous solids (Raleigh et al., 1988, 1989; Levitt et al., 1990; Creuzet et al., 1991a,b). This method is based on the fact that homonuclear dipolar couplings in solids, which are ordinarily attenuated by magic angle sample rotation, are partially reintroduced when the spinning rate satisfies the rotational resonance condition—$\delta = n\omega_r/2\pi$, where δ is the isotropic shift separation, $\omega_r/2\pi$ is the spinning speed, and n is a small integer denoting the order of the resonance. The recoupling which occurs at rotational resonance can lead to dramatic changes in the line shape of both spins and to very efficient exchange of magnetization within the spin pair. Simulations of the magnetization exchange trajectories at rotational resonance have proven to be an accurate means of extracting the intrapair distance up to 5.0 Å (Raleigh et al., 1989; Creuzet et al., 1991b). The virtue of this approach as a probe of protein structure is that it represents no constraints on the solubility of the protein nor on its tendency to crystallize. This kind of measurement may therefore open the door for accurate structural determinations of membrane proteins and other species where structural studies are problematic (McDermott et al., 1990).

Recently, we described the first rotational resonance measurement of a carbon–carbon distance in a protein—in particular, in double ^{13}C-labeled retinal bound to bR[1] (Creuzet et al., 1991a). This study addressed the conformation of the retinal about the 6-s bond in bR, which has great relevance for quantitatively assessing contributions to the opsin shift. The first indications from chemical shift measurements favored

† This research was supported by the National Institutes of Health (GM-23289, GM-36801, GM-36920, and RR-00995), the Netherlands Foundation for Chemical Research (SON), and the Netherlands Organization for the Advancement of Pure Science (NWO). A.E.M. was supported by an American Cancer Society Fellowship (PF-2383) and F.C. by an MIT Bantrell Fellowship.

‡ Massachusetts Institute of Technology.

§ Present address: Department of Chemistry, Columbia University, 116th and Broadway, New York, NY 10027.

⊥ Present address: Unité Mixte de Recherche, CNRS/Saint Gobain, 39 Quai Lucien Lefranc, 93303 Aubervilliers Cedex, France.

∥ Rijksuniversiteit te Leiden.

⊛ Stockholm University.

▽ Brandeis University.

⊛ Abstract published in *Advance ACS Abstracts,* November 15, 1993.

[1] Abbreviations: bR, bacteriorhodopsin; CSA, chemical shielding anisotropy; MAS, magic angle spinning; NMR, nuclear magnetic resonance; SS NMR, solid-state nuclear magnetic resonance.

0006-2960/94/0433-6129$04.50/0

Scheme I

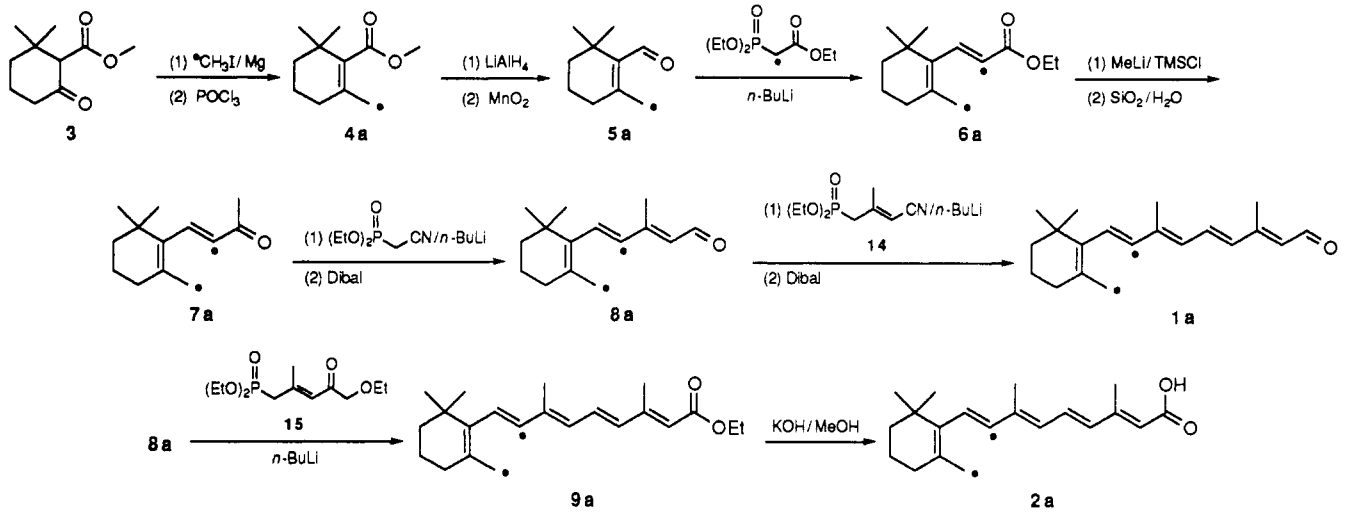

a 6-s-*trans* conformation and, at the same time, indicated strong perturbations from the local environment (Harbison et al., 1985a, 1985b). In pursuing internuclear distances about the 6-s bond, we placed the chemical shift interpretation on a more secure foundation. Moreover, having assessed the method's promise for biological systems, we plan a series of accurate measurements of intra- and intermolecular distances in bR that will address a variety of unresolved issues relevant to the opsin shift, the structure of the retinal binding pocket, and the mechanism of proton pumping.

From the viewpoint of NMR methodology these measurements of distances about the 6-s bond in the retinal of bR deserve more careful inspection. To make a convincing case for this new structural method we have measured additional distances so that there is some redundancy, and, therefore, less ambiguity in our data. In addition, we have further delineated the spectral parameters that are necessary for obtaining a distance from simulations of the magnetization transfer data. Finally, we have explored the possibility of bond angle determination by this method which might have many applications as a new approach for defining the relative orientations of two groups in a membrane protein. We intend the present discussion as a type of practical guide for biological measurements via this new method. At the moment, it appears promising for the measurement of ^{13}C–^{13}C distances up to approximately 6.0 Å, with an accuracy of approximately 0.4 Å or less, utilizing only data that are readily obtain by standard solid-state NMR methods.

MATERIALS AND METHODS

Synthesis of [8,18-$^{13}C_2$]Retinal and [8,18-$^{13}C_2$]Retinoic Acid. The synthesis of [8,18-$^{13}C_2$]retinal (**1a**) and [8,18-$^{13}C_2$]retinoic acid (**2a**), both with 93% $^{13}C_2$ incorporation, is summarized in Scheme I. Keto ester **3**, prepared according to literature procedures (Spijker-Assink et al., 1988; White et al., 1985) is used as the starting compound. A Grignard reaction of ^{13}C-labeled methylmagnesium iodide with **3**, followed by dehydration of the tertiary alcohol with $POCl_3$ in pyridine, gives the unsaturated ^{13}C-labeled ester **4a** in 38% yield after purification. Reduction of the ester function with lithium aluminum hydride and subsequent oxidation of the allytic alcohol function with manganese dioxide leads to ^{13}C-labeled β-cyclocitral (**5a**) in 60% yield. A Horner–Emmons reaction between **5a** and [2-^{13}C]triethyl phosphonoacetate, synthesized in 92% yield from [2-^{13}C]ethyl bromoacetate and triethyl phosphite, using *n*-butyllithium as a base, affords the $^{13}C_2$-labeled ester **6a** in 81% yield. Reduction methylation of the ester function with methyllithium in the presence of chlorotrimethylsilane (Cooke, 1986) gives the $^{13}C_2$-labeled β-ionone (**7a**) in 82% yield, after acidic workup. **7a** is reacted in a Horner–Emmons reaction with diethyl(cyanomethyl)-phosphonate, using *n*-butyllithium as a base, followed by a Dibal reaction, leading to $^{13}C_2$-labeled β-ionylideneacetaldehyde (**8a**). This C_{15}-aldehyde is converted into [8,18-$^{13}C_2$]-retinal (**1a**) by a Horner–Emmons coupling with C_5-phosphonate **14**, using *n*-butyllithium as a base, followed by a Dibal reduction. Based on **7a**, the yield of retinal (**1a**) is 64% (Pardoen et al., 1985). The all-*trans* isomer is isolated in pure form by column chromatography.

The analytical data completely support the structure of all-*trans* retinal (**1a**). Mass spectroscopy gives an exact mass of 286.2193 (calcd for $^{12}C_{18}{}^{13}C^2H_{28}O$, 286.2208); the $^{13}C_2$ incorporation is 93% (94% on position 18 and 99% on position 8). The ^1H–^1H coupling constants and the chemical shift values in the 200-MHz ^1H-NMR spectrum are identical to those of all-*trans* retinal (Patel, 1969).[2] In addition, ^{13}C–^1H splittings are observed,[1] showing that the ^{13}C-label is on the 8 and 18 position. The intensities confirm the high ^{13}C incorporation found by mass spectroscopy. The ^1H noise-decoupled, 50-MHz ^{13}C-NMR spectrum is dominated by two strong peaks at the chemical shift values known for C-8 (137.07 ppm) and C-18 (21.77 ppm) in all-*trans* retinal (Englert, 1975).[3] In addition, ^{13}C–^{13}C coupling constants are observed.[2]

The all-*trans* [8,18-$^{13}C_2$]retinoic acid (**2a**) is obtained from C_{15}-aldehyde **8a** in two steps: Horner–Emmons reaction of C_{15}-aldehyde **8a** with C_5-phosphonate **15**, using BuLi as a base, gives the C_5-elongated ethyl retinoate (**9a**), and

[2] ^1H-NMR (200 MHz, $CDCl_3$) of 8,18-$^{13}C_2$-retinal (**1a**): δ 1.04 (s, 16-H + 17-H), 1.45 (m, 2-H), 1.60 (m, 3-H), 1.72 (d, $^1J_{CH}$ = 123 Hz, 18H), 2.0 (m, 4-H), 2.03 (d, $^3J_{CH}$ = 4 Hz, 19H), 2.33 (s, 20H), 5.96 (d, J_{HH} = 8 Hz, 14-H), 6.16 (dd, $^1J_{CH}$ = 155 Hz, J_{HH} = 16 Hz, 8-H), 6.19 (dd, J_{HH} = 11 Hz, $^3J_{CH}$ = 9 Hz, 10-H), 6.34 (d, J_{HH} = 16 Hz, 7-H), 6.37 (d, J_{HH} = 15 Hz, 12-H), 7.14 (dd, J_{HH} = 11, 15 Hz, 11-H), 10.11 (d, J_{HH} = 8 Hz, 15-H) ppm.

[3] ^{13}C-NMR (50 MHz, $CDCl_3$) of 8,18-$^{13}C_2$-retinal (**1a**): δ 13.02 (19-C), 13.12 (20-C), 19.19 (3-C), 21.77 (enriched, 18-C), 28.97 (16/17-C), 33.15 (4-C, $^2J_{CC}$ = 3 Hz), 34.27 (1-C, $^3J_{CC}$ = 3 Hz), 39.59 (2-C), 128.99 (14-C), 129.38 (10-C), 129.71 (7-C, $^1J_{CC}$ = 71 Hz, $^3J_{CC}$ = 4 Hz), 130.51 (5-C, $^1J_{CC}$ = 44 Hz, $^3J_{CC}$ = 5 Hz), 132.54 (11-C, $^3J_{CC}$ = 7 Hz), 134.50 (12-C), 137.07 (enriched, 8-C), 137.62 (6-C), 141.29 (9-C, $^1J_{CC}$ = 54 Hz), 154.81 (13-C), 191.12 (15-C) ppm.

Scheme II

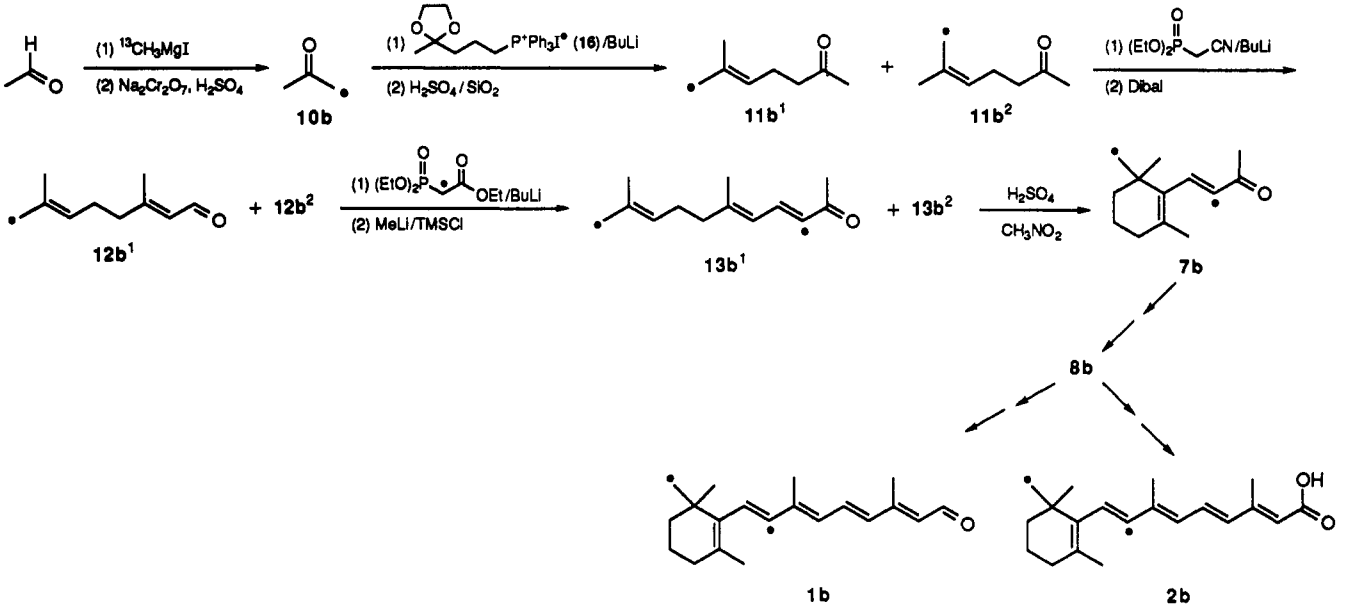

saponification of **9a** with a 10% solution of potassium hydroxide in methanol under reflux conditions results in retinoic acid (**2a**) in 79% yield. The all-*trans* isomer can be separated by column chromatography. The spectral data are completely in agreement with the all-*trans* [8,18-$^{13}C_2$]retinoic acid (**2a**).

Synthesis of [8,16-$^{13}C_2$]Retinal and [8,16-$^{13}C_2$]Retinoic Acid. The synthesis of [8,16-$^{13}C_2$]retinal (**1b**) and [8,16-$^{13}C_2$]retinoic acid (**2b**) is summarized in Scheme II. Acetic aldehyde is used as the starting compound. A Grignard reaction with ^{13}C-labeled methylmagnesium iodide, followed by a Jones oxidation of the secondary alcohol function, results in [1-^{13}C]acetone (**10b**) in 75% yield. Wittig reaction of **10b** with phosphonium salt **16** (Gebhard et al., 1989), using *n*-BuLi as a base, followed by acidic hydrolysis of the dioxolane ring, leads to 6-methyl-5-hepten-2-one, in a 61% yield. As expected, this ketone appears in two isotopomeric forms: [7-^{13}C]-6-methyl-5-hepten-2-one (**11b^1**) and [6-$^{13}CH_3$]-6-methyl-5-hepten-2-one (**11b^2**) are the result of the Wittig reaction with the asymmetrically-labeled acetone. **11b** is reacted in a Horner–Emmons reaction with diethyl(cyanomethyl)phosphonate, using *n*-BuLi as a base, followed by a Dibal reduction of the nitrile function, to produce ^{13}C-labeled 3,7-dimethyl-2,6-octadienal (**12b**), again in two isotopomeric forms, in 62% yield. A Horner–Emmons reaction of **12b** and [2-^{13}C]triethyl phosphonoacetate (see above), using *n*-BuLi as a base, gives after reductive methylation of the ester function the 13C-labeled pseudoionone **13b** in a 48% yield, still in two isotopomeric forms. Cyclization of **13b** with sulfuric acid in nitromethane results in $^{13}C_2$-labeled β-ionone (**7b**) in an 88% yield. β-Ionone (**7b**) is not a mixture of two isotopomers; instead, it is a racemic mixture of two enantiomeric β-ionones. β-Ionone (**7b**) has been converted into [8,16-$^{13}C_2$]retinal (**1b**) and [8,16-$^{13}C_2$]retinoic acid (**2b**), as described previously for [8,18-$^{13}C_2$]retinal (**1a**) and [8,18-$^{13}C_2$]retinoic acid (**2a**).

The analytical data are completely in agreement with the structure of all-*trans* retinal (**1b**): the exact mass measured by mass spectroscopy is 286.2200 (calcd for $^{12}C_{18}{}^{13}C_2H_{28}O$, 286.2208); the $^{13}C_2$ incorporation is 98% (99% on each position). The 200-MHz ^1H-NMR spectrum is identical to that of all-*trans* retinal (Patel, 1969).[4] In addition, ^{13}C–^1H splittings are observed,[3] confirming the positions of the labels. In the 50-MHz ^{13}C-NMR spectrum, two strong peaks are observed at the C-8 position (137.04 ppm) and at the C-16 position (28.94 ppm).

NMR Spectroscopy. Doubly-labeled retinoic acid was diluted 5-fold into natural abundance retinoic acid (Sigma Chemical Co., St. Louis, MO) and then recrystallized in the monoclinic and triclinic forms as described previously (Harbison et al., 1985a). Regeneration of bR with doubly-labeled retinal followed a previously described protocol (McDermott et al., 1990).

NMR spectra were recorded on home-built spectrometers and utilized probes with high-speed rotors and stators obtained from Doty Scientific (Columbia, SC). Typical 90° pulse widths were 3 and 4 μs for ^1H and ^{13}C, respectively. The pulse sequence for rotational resonance experiments is a standard Z-magnetization transfer sequence and was explicitly described in previous applications (Raleigh et al., 1988; McDermott et al., 1990; Levitt et al., 1990; Creuzet et al., 1993).

For the bR studies, identical control experiments were performed using natural abundance bR, and in each case, the scaled subtraction of the labeled and natural abundance spectra was used for analysis. Analyses of both the retinoic acid data and the bR difference spectra were performed by recording the line intensities for both labeled carbons from spectra processed with a large exponential line broadening (50 Hz). The set of intensities (for various mixing time points) for each site was scaled with the zero-mix times normalized to 1.0 for the C-8 and −1.0 for the methyl carbon. The difference in intensities for the two spins was then computed for each mixing time, and half this value was then plotted for comparison with simulations.

The algorithm for simulating the magnetization exchange trajectories has been described in detail elsewhere (Levitt et al., 1990; Creuzet et al., 1994). Briefly, the program calculates the time evolution of a two-spin system under the presence of

[4] ^1H-NMR (200 MHz, $CDCl_3$) of 8,16-$^{13}C_2$-retinal (**1b**): δ 1.03 (d, $^1J_{CH}$ = 126 Hz, 16-H), 1.03 (d, $^3J_{CH}$ = 5 Hz, 17-H), 1.4–1.7 (m, 2-H + 3-H), 1.72 (s, 18-H), 2.0 (m, 4-H), 2.3 (d, $^3J_{CH}$ = 3 Hz, 19-H), 2.33 (s, 20-H), 5.97 (d, J_{HH} = 8 Hz, 14-H), 6.16 (dd, $^1J_{CH}$ = 155 Hz, J_{HH} = 16 Hz, 8-H), 6.1–6.5 (m, 7-H + 10-H), 6.37 (d, J_{HH} = 15 Hz, 12-H), 7.15 (dd, J_{HH} = 15 Hz + 12 Hz, 11-H), 10.10 (d, J_{HH} = 8 Hz, 15-H) ppm.

Table I: Internuclear Distances and Angles α_S and β_S Derived from NMR

compd	internuclear distance (Å)	β_S	α_S
8,18			
6-s-*cis* (triclinic) retinoic acid	2.9 ± 0.2 (3.1)[a]	42 ± 5° (48°)[a]	nd[c]
6-s-*trans* (monoclinic) retinoic acid	4.0 ± 0.2 (4.2)[a]	90 ± 15° (90°)[a]	0 ± 40° (40°)[a]
bR	4.1 ± 0.2	nd	nd
8,16(17)			
bR	3.4 ± 0.2[b]	nd	nd

[a] Distances derived from crystal structure coordinates for triclinic and monoclinic retinoic acid (Stam, 1972; Stam & MacGillavry, 1963). [b] Retinoic acid in the 6-s-*trans* form has 3.2- and 3.4-Å distances for the 8–16 and 8–17 positions, respectively, and for the 6-s-*cis* form the distances are 4.0 and 4.3 Å, respectively. [c] nd, not determined.

Table II: Anisotropic Chemical Shift Parameters Employed for the Simulations Described in the Text

functional group	6-s-*trans*	6-2-*cis*
methyl (C-18)[a]		
σ_{iso}	24 ppm	21 ppm
δ	19 ppm	12 ppm
η	0.87	0.85
Euler angles (α, β, and γ)[b]	–27°, 20°, 29°	40°, –24°, –35°
polyene (C-8)		
σ_{iso}	139 ppm	131 ppm
δ	106 ppm	111 ppm
η	0.90	0.86
Euler angles (α, β, and γ)[c]	–82°, 162°, 38°	43°, 89°, 37°

[a] Parameters for C-16 and C-17 in bR were as above for 6-s-*cis*, except that σ_{iso} = 29 ± 1 ppm in approximate agreement with model compounds (Harbison et al., 1985b). [b] Euler angles (Spiess, 1978) assuming that σ_{xx}, the most shielded element, is along the C–C bond. [c] Euler angles (Spiess, 1978) assuming that σ_{xx}, the most shielded element, is perpendicular to the polyene plane and σ_{yy}, the intermediate value, is along the C=C bond.

a time-dependent Hamiltonian by numerical integration, using discrete time elements short in comparison to the rotor cycle. Necessary input parameters are the principal values of chemical shielding tensors for both sites and their relative orientations, the distance, the relaxation time of the zero-quantum transition (T_2^{ZQ}), and the dipolar tensors relative to a crystal-fixed frame. In general, five angles are necessary to specify all the relative interaction tensor orientations: an angle β_S specifying the angle between the largest shielding element of the S spin and the internuclear axis, an angle α_S specifying the orientation of the other two shielding elements of the S-spin with respect to this axis, two angles β_I and α_I for the I-spin, and an angle $\Delta\gamma$, the dihedral angle around the internuclear axis for the largest principal shielding elements of the two spins. However, if the shielding anisotropy of one of the spins in the pair is small, as is the case here for the I spin, then the dependencies of the spin dynamics on the angles β_I and α_I and $\Delta\gamma$ are weak.

For the simulations we utilized distances derived from retinoic acid crystal structures (see Table I) (Stam, 1972; Stam & MacGillavry, 1963) together with tensor orientations from previous single-crystal NMR characterizations of similar chemical moieties (Wolff et al., 1977; Mehring, 1983). Accurate CSA parameters were obtained from MAS spectra at rotation frequencies between 3.0 and 3.5 kHz by previously described procedures (Herzfeld and Berger, 1980). These data are compiled in Table II. T_2^{ZQ} was estimated by the convolution of the two line widths; in particular, $1/T_2^{ZQ} = \pi(\Delta_1 + \Delta_2)$, where Δ_1 and Δ_2 refer to the line widths of the individual peaks (full width at half-height, measured in Hz). For the retinoic acid samples, the [8,18-^{13}C]retinal-bR, and the [8,16(17)-^{13}C]retinal-bR, these values were 5.2, 1.8, and 1.1 ms, respectively.

The contour plots of T_2^{ZQ} versus dipolar coupling shown below were constructed from a family of trial simulations in which the values for two fitting parameters of interest are stepped through all combinations of chosen trial values. To speed up the simulations, an analytical approximation for the magnetization exchange dynamics was used (Levitt et al., 1990). The errors generated by this approximation have been shown to be small in the regime considered here. In Figure 2 we display contour lines for constant rms deviation between the magnetization exchange data and the simulation (Creuzet et al., 1994). The minima in these contours represent regions of best fit in the variable parameter space. The contour lines are drawn in all cases at the following rms values (Creuzet et al., 1994): solid lines are at 0.2 and 0.5, heavily dashed lines are at 0.1, lighter dashed lines at 0.08, and dotted lines at 0.06 and 0.05.

RESULTS

Retinoic Acid. Magnetization transfer trajectories have been measured for 6-s-*cis* and 6-s-*trans* forms of retinoic acid (the triclinic and monoclinic crystal forms, respectively) for the first three orders of rotational resonance. In these experiments, the spinning speed is chosen to match the rotational resonance condition, and then magnetization exchange is measured using a pulse sequence that aligns both spins along Z, selectively inverts one spin, waits for variable periods (the mixing times indicated in Figure 1), and then detects the remaining Z-magnetization with a readout pulse. Along with these data in Figure 1 we show a simulation of the expected magnetization transfer curve, calculated using known parameters from the crystal structure as described in the Materials and Methods. It is clear that this approach leads to good simulations for all of the experimental data when the structure of the compound is well characterized. In the following discussion we would like to explore the dependencies of the simulations on all of the above parameters to elucidate which parameters are crucial to the determination of accurate bond distances and which are of less importance. Such a study was motivated by our interest in applying this method to progressively less well-characterized systems.

In Figure 2 we show the dependence of the quality of the simulation on the choice of the dipolar coupling and the T_2^{ZQ} as described in the Materials and Methods. The most significant observation from these plots is that there is a unique minimum from which we can reliably estimate error bounds. The second conclusion is that, for these exchange trajectories, the value determined for the dipolar coupling (hence, the internuclear distance) is fairly independent of choice of the relaxation time. Analogous contour plots were constructed to evaluate the covariance of the dipolar coupling and the tensor parameters for the $n = 1$ conditions. Such plots showed very little dependence for the distance determination on tensor breadth and essentially no dependence on tensor asymmetry and orientation for both members of the spin pair. We conclude that in this regime of moderate dipolar couplings it

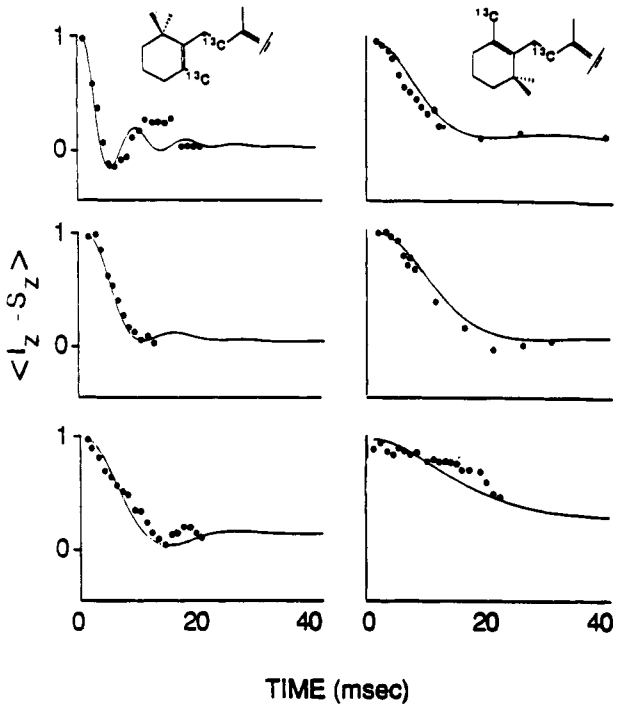

FIGURE 1: Magnetization transfer curves for the [8,18-$^{13}C_2$] retinoic acid crystallized in the 6-s-*cis* (triclinic) and 6-s-*trans* (monoclinic) forms are displayed in the left- and right-hand columns, respectively. The $n = 1, 2, 3$ resonance conditions are shown (top to bottom), with experimental values as black dots and simulations as solid lines. The dipolar couplings used in the simulations were 255 and 103 Hz, respectively, and Euler angles were derived from their crystal coordinates.

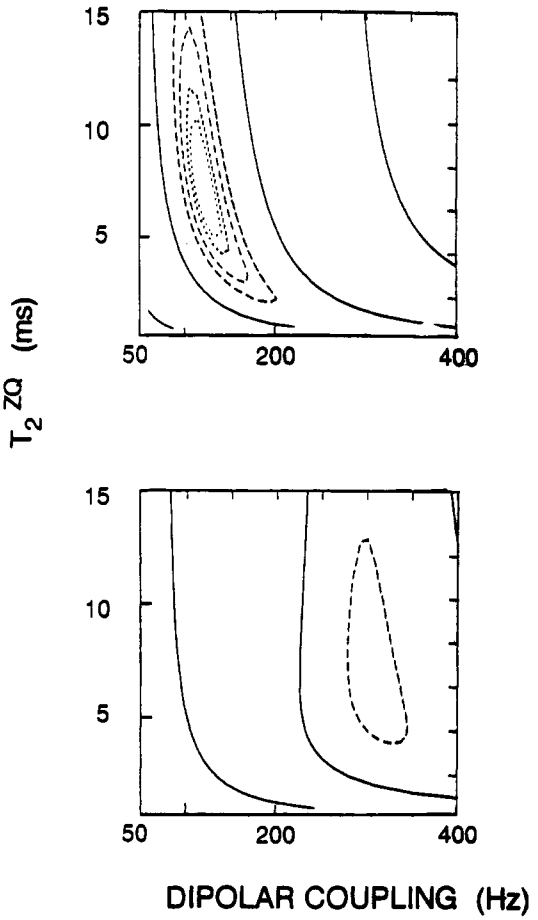

FIGURE 2: Contour lines, describing regions of equal rms deviation between simulation and data, are indicated as a function of the dipolar coupling and the relaxation time used in the simulation. Note that for the $n = 1$ data of 6-s-*cis* (bottom) and 6-s-*trans* (top) retinoic acid, which is labeled at the C-8 and C-18 carbons, a single, well-defined minimum in the fit is obtained which is strongly dependent on the dipolar coupling and weakly dependent on the relaxation parameter assumed.

is not essential to determine the tensor parameters to a high degree of precision in order to measure the bond distance accurately, and it is sufficient to estimate the relaxation rates by measuring the line widths as described in the Materials and Methods. Thus, the signal-to-noise ratio in the intensity measurements is the limiting factor in our ability to determine the distances from $n = 1$ data.

For the higher orders of rotational resonance ($n = 2, 3, ...$), rotational sidebands appear in the spectra. Since these reflect the molecular orientation of the shift tensors, it is reasonable that the magnetization exchange trajectories may now depend on tensor orientations. Of all these orientational parameters, the most dramatic dependence consistently arises from the Euler angle, β_s, where S refers to the spin in the IS pair with the larger anisotropy (in our systems S refers to the 18-^{13}C and I to the methyl ^{13}C at position 16, 17, or 18 in the different labeled compounds). As illustrated in Figure 3, this angle describes the angle subtended between the internuclear vector and the σ_{zz} direction of the chemical shift tensor. Frequently, this latter direction will correspond to a chemically relevant direction such as an axis of high symmetry, since it is likely to be electronically the most unique. For the 8-^{13}C of retinal this direction is perpendicular to the polyene plane, and the angle β_S thus describes the angle between this perpendicular and the 8-^{13}C–18-^{13}C internuclear vector. As illustrated in Figure 3, this angle is directly related to whether the double bond of the ionone ring is conjugated with the polyene. We comment that there is a large difference in the expected values of β_S for the 6-s-*cis* and 6-s-*trans* conformations. The steric interaction between the 18-^{13}C methyl group and the proton attached to 8-^{13}C leads to a skewed 6-s-*cis* conformation forced out of conjugation. In contrast, the 16-C–17-C methyl groups are locked around the 8-C proton in the 6-s-*trans* conformation, and the polyene normal is perpendicular to the internuclear vector, yielding $\beta_S = 90°$. Simulations show a very strong dependence of the quality of fit on the value of β_S, with the best simulations being very close to the crystallographically derived values. After this angle, the three next most influential angles were α_S, β_S, and $\Delta\gamma$, in descending order of importance for our particular case. In Figure 3 we display the effects of the values of β_S and α_S on the rms deviation of the magnetization exchange simulation. In these simulations the dipolar coupling has been fixed to the value determined from the analysis of the $n = 1$ data (which is in agreement with the value expected from crystallographically known distances), and all other angles have been fixed to the crystallographically known values.

The other angles, α_I and $\Delta\gamma$, have relatively little influence on the quality of the fit and, hence, could alternatively have been set to arbitrary values. The more shallow minimum for the determination of β_S in the 6-s-*trans* conformer is due to additional dependence on the value for α_S. As β_S approaches 0°, in the limit that the other site has negligible asymmetry (as in the case for a methyl group), there will be no dependence on the values for the other Euler angles, since they only describe the orientation of chemical shielding tensor elements perpendicular to the dipolar axis. However, in the limit of $\beta_S = 90°$ these other angles may influence the quality of fit, as seen for the 6-s-*trans* conformation. Here the minimum is described by an ellipse, showing evidence of a stronger dependence on β_S than on α_S, with the extreme values at $\beta_S = 90°$, $\alpha_S = 40°$,

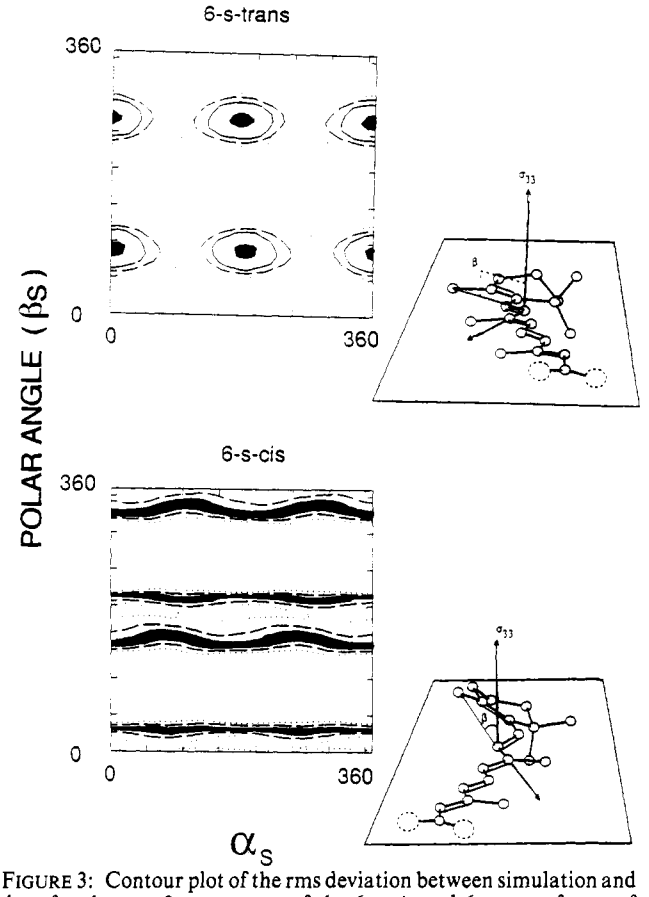

FIGURE 3: Contour plot of the rms deviation between simulation and data for the $n = 2$ resonances of the 6-s-*cis* and 6-s-*trans* forms of retinoic acid, where the dipolar coupling and relaxation parameters have been fixed to the correct values, and the Euler angles β_S and α_S are varied. For the 6-s-*cis* conformation (bottom) a unique minimum occurs at 43° (the darkened region), and for symmetry-related values for β_S, while essential, no dependence on α_S is seen. In contrast, for the 6-s-*trans* form the rms deviation depends somewhat on both angles so our error is larger. Alongside the contour plots are perspective drawings of the planar 6-s-*trans* retinal, and the out-of-plane 6-s-*cis* structure. The value β_S that is readily derived from simulation of the $n = 2$ curves is the angle between the R_{zz} vector for the C-8 and the internuclear vector. The value for β_S is approximately 90° minus the degree of dihedral rotation about the 6–7 bond that destroys conjugation of the ring alkene into the polyene.

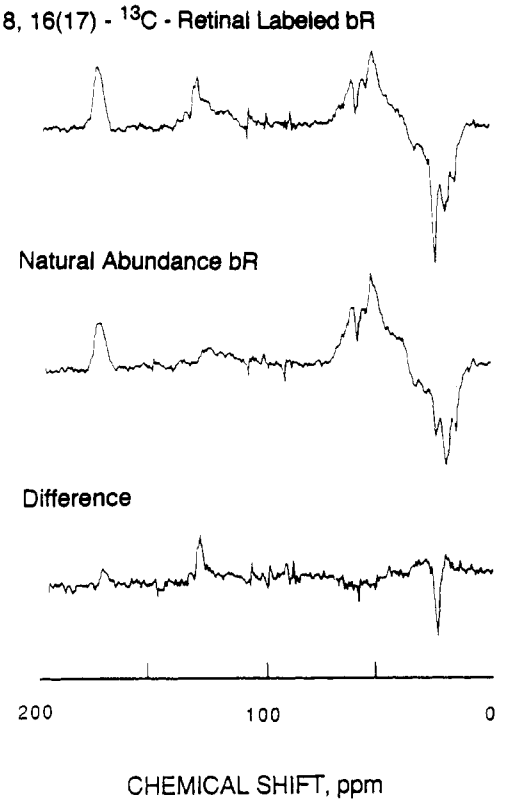

FIGURE 4: ^{13}C difference spectra for [8,16(17)-^{13}C]retinal-bR collected using a Z-magnetization exchange pulse sequence with zero mixing time. The sample may be thought of as a 50:50 mixture of [8,16-$^{13}C_2$]- and [8,17-$^{13}C_2$]retinal-bR. Intensities derived from such data (with variable mixing times during decoupling) were used to construct the transfer curve shown in Figure 6.

and $\beta_S = +15°$, $\alpha_S = 0°$. The latter is unlikely as a possibility, since $\alpha_S = 0°$ and $\gamma_S = 0°$ only occur if the dipolar axis coincides with the polyene direction, which is not the case here. Indeed, the solution $\beta_S = 90°$, $\alpha_S = 40°$ is not only indicated by simple geometric arguments but is also the result calculated from the crystal structure coordinates.

This choice of variable parameters illustrates what we conceive as a useful recipe for determining local structures. Initially, the internuclear distance can be determined by fitting $n = 1$ data using relaxation rates and tensor parameters as determined from off-rotational resonance MAS spectra. If the sideband intensities are small, at $n = 1$, then the distance is essentially independent of the tensor orientations. In a second experiment, $n = 2$ data are simulated using the distance determined from the $n = 1$ analysis and the relaxation parameter and the CSA chosen for the $n = 1$ experiment; the simulation of $n = 2$ will particularly constrain the value for β_S for the site with the largest shielding anisotropy, which frequently has a meaningful chemical interpretation. We note also that this approach to measuring the orientation of the 8-C tensor is much more sensitive to the rotation about the 6–7 bond and the breaking of conjugation than would be an $n = 1$ distance measurement. The detailed analyses of the $n = 3$ data (not shown here) also support these values for the polar angle, but thus far, our analyses of $n = 3$ do not offer a more precise determination of any additional angles. The results of this analysis for the two forms of retinoic acid are included in Table I.

Bacteriorhodopsin. We have measured two magnetization transfer curves in bR that are important for determining the conformation about the 6-s bond of the retinal bound to the protein. For these experiments the large natural abundance ^{13}C background in bR necessitates the use of difference spectra. Figure 4 illustrates the difference spectrum for the zero mixing time point for the measurement of the 8–16(17) distance in bR. From a family of such difference spectra, collected with variable mixing times, we obtain the data displayed in Figure 5, which are presented along with the curves calculated for the 6-s-*cis* and 6-s-*trans* conformations. For the simulations in Figures 5 we have used an estimate for T_2^{ZQ} that is based on the measured line widths. Since this parameter has a substantial influence on the simulations, we discuss it in the following section. However, there is no value of T_2^{ZQ} for which it is possible to produce an adequate simulation of all the experimental results using structural parameters characteristic of the 6-s-*cis* conformer. In other words, the data are only consistent with a 6-s-*trans* conformation, even if one questions our estimate for T_2^{ZQ} and the Euler angles. Interestingly, the distances that are well accepted from the 6-s-*trans* model compounds correlate exactly with our estimate for T_2^{ZQ} based on line width, suggesting that we are estimating T_2^{ZQ} correctly. In Figure 6 we illustrate the dependencies of the quality of fits on the dipolar coupling and the value for β_S. The derived dipolar coupling corresponds to a well-defined, unique minimum with no dependence on β_S and an 8–16(17)

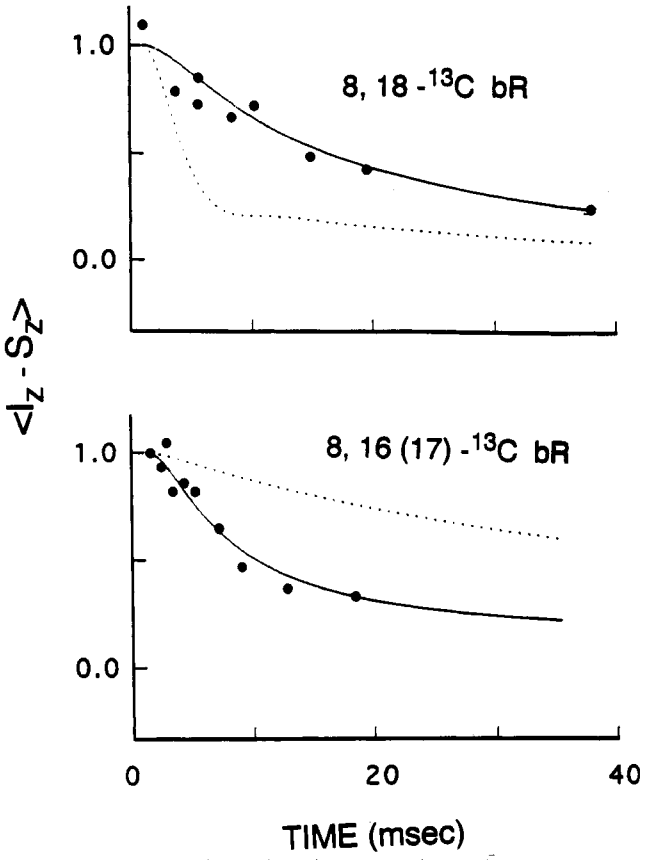

FIGURE 5: Measured (dots) and calculated (lines) magnetization exchange trajectories for [8,18-^{13}C]retinal-bR and [8,16(17)-^{13}C]-retinal-bR. The expected curves for the 6-s-*cis* (dashed lines) and 6-s-*trans* (solid lines) conformations were computed using the distances and orientations from the retinoic acid analysis and the relaxation times, determined from the bR line widths. For the 8,-18-labeled sample these correspond to dipole couplings of 225 and 103 Hz; for the 8,16(17) the couplings are 90 and 202 Hz.

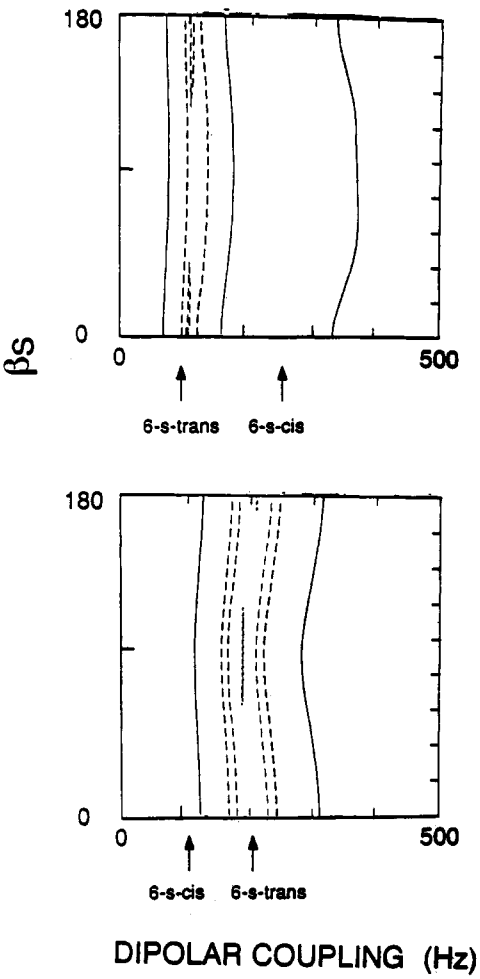

FIGURE 6: Contour plot displaying the dependence of the rms deviation between data and simulation of the $n = 1$ magnetization transfer curves for [8,18-$^{13}C_2$]retinal-bR (top) and [8,16(17)-$^{13}C_2$]-retinal-bR (bottom). In this grid the dipolar coupling and the Euler angle, β_S, describing the orientation of the C-8 tensor are varied. This illustrates that the orientation of the tensor is unnecessary for a precise determination of the internuclear distance. Arrows at the bottom of the diagram indicate the expected dipolar couplings based on the crystallographic distance. (Other Euler angles show even less sensitivity; data not shown.)

distance of 3.4 ± 0.2 Å (Table I). In contrast, preliminary data obtained for an $n = 2$ transfer curve exhibit a dependence on the orientation of the 8-C tensor relative to the dipolar axis. In future investigations we plan to pursue these measurements with greater accuracy.

DISCUSSION

We describe a new method for measuring distances in polycrystalline and amorphous solids that yields accurate and reliable results, even when the dipolar coupling is less than the NMR line width. The simulations of the magnetization transfer curves require knowledge of the chemical shift anisotropies and accurate measurement of the line width of both spins. Knowledge of the orientation of the tensors is not necessary for most cases because at the $n = 1$ condition the transfer curves are fairly independent of orientation. Indeed, we illustrate that some information about the orientations may be derived from this method if both $n = 1$ and higher-order resonances ($n = 2$, 3, etc.) are measured and simulated with consistent values. However, the distance measurement is sensitive to the estimate of the relaxation rate for the zero-quantum state, T_2^{ZQ}, which we derive from the line widths. With this approach we have obtained consistent results for many compounds of known structure, and for the first time we discuss simulations for biological systems with broader lines and uncharacterized broadening mechanisms (*vide infra*).

Small systematic errors in the distances might occur for the model compounds such that our derived distances are biased short, as compared with crystallographically known values by approximately 0.1–0.2 Å. We cannot yet conclude whether this is significant, as compared with random errors, nor do we know whether it will occur generally. This phenomenon could be due to vibrational averaging that occurs differently in a dipolar coupling as compared with a crystallographic distance measurement. Whatever their cause, these deviations do not exceed our estimated precision.

Because of the weak coupling and broad lines, the distance we obtain for the bR samples depends somewhat on the value for T_2^{ZQ}. As described above, we have obtained T_2^{ZQ} from the line widths. Contributions to the line widths observed in a biological sample are rather uncharacterized and presumably include proton couplings that are incompletely averaged and inhomogeneous splittings due to the local environments. In the case where the dephasing for the two sites is independent and can be expressed in terms of a rapidly fluctuating interactions in the Redfield relaxation limit, our method for estimating T_2^{ZQ} should be sound. It is likely that this assumption of uncorrelated sites is warranted; however, we have in these data inherent proof that it is a good assumption by means of the following arguments. For both measurements in bR, it is very clear that we must rule out the distance typical

of 6-s-*cis* conformations on the basis of fit quality alone, regardless of the assumed values for T_2^{ZQ}. Therefore, we assume that bR must be in a 6-s-*trans* conformation and assume that it must be characterized by distances that are well accepted from 6-s-*trans* model compounds. The distance derived from the rotational resonance method agrees well with the distance from such model compounds *only if* the T_2^{ZQ} values used in the simulations are approximately equal to the value we obtained based on line widths. This is a strong argument that we are estimating T_2^{ZQ} correctly. In addition, we note that in view of the possibility of drift in the line widths with such long signal averaging times, it is important that this line width be repeatedly checked for successive spectra.

We have demonstrated that after the internuclear distance is derived from $n = 1$ data the higher orders can be used to derive partial information about the orientations of the groups. In this example this orientational information could be approximately related to the angle of rotation of the 6–7 bond and, therefore, to the degree to which conjugation is broken. If one looks to other interesting systems that are amenable to analysis by rotational resonance, the angle β_S may frequently have an important chemical interpretation, since it describes the orientation (relative to the internuclear axis) of the largest principal shielding element of the site with the largest CSA. This exciting, new ability to determine conformation angles could also be applied in principle to questions of strain about dihedral angles in a variety of other systems.

ACKNOWLEDGMENT

The authors would like to thank K. V. Lakshmi for technical assistance and helpful suggestions.

REFERENCES

Cooke, M. P., Jr. (1986) *J. Org. Chem. 51*, 951.

Creuzet, F. J., McDermott, A. E., Gebhard, R., van der Hoef, K., Spijker-Assink, M. B., Herzfeld, J., Lugtenburg, J., Levitt, M. H., & Griffin, R. G. (1991a) *Science 251*, 783.

Creuzet, F. J., Raleigh, D. P., Levitt, M. H., & Griffin, R. G. (1992) *J. Am. Chem. Soc.* (in press).

Englert, G. (1975) *Helv. Chim. Acta 58*, 2367.

Gebhard, R., Courtin, J. M. L., Shadid, J. B., van Haveren, J., van Haeringen, C. J., & Lugtenburg, J. (1989) *Recl. Trav. Chim. Pays-Bas 108*, 107.

Harbison, G. S., Smith, S. O. Pardoen, J. A., Courtin, J. M. L., Lugtenburg, J., Herzfeld, J., Mathies, R. A., & Griffin, R. G. (1985a) *Biochemistry 24*, 6955–6962.

Harbison, G. S., Mulder, P. P. J., Pardoen, J. A., Lugtenburg, J., Herzfeld, J., & Griffin, R. G. (1985b) *J. Am. Chem. Soc. 107*, 4809–4816.

Herzfeld, J., & Berger, A. E. (1980) *J. Chem. Phys. 73*, 6021–6030.

Levitt, M. H., Raleigh, D. P., Creuzet, F., & Griffin, R. G. (1990) *J. Chem. Phys. 92*, 6347–6364.

McDermott, A. E., Creuzet, F., Griffin, R. G., Zawadzke, K. E., Ye, Q.-Z., & Walsh, C. T. (1990) *Biochemistry 29*, 5767–5775.

McDermott, A. E., Thompson, L. K., Pelletier, S., Farrar, M. R., Winkel, C., Lugtenburg, J., Herzfeld, J., & Griffin, R. G. (1991) *Biochemistry* (submitted for publication).

Mehring, M. (1983) *Principles of High-Resolution NMR in Solids*, pp 250–257, Springer-Verlag, Berlin.

Pardoen, J. A., Winkel, C., Mulder, P. P. J., & Lugtenburg, J. (1984) *Recl. Trav. Chim. Pays-Bas 103*, 135.

Pardoen, J. A., Mulder, P. P. J., van den Berg, E. M. M., & Lugtenburg, J. (1985) *Can. J. Chem. 63*, 1431.

Patel, D. (1969) *Nature (London) 221*, 825.

Raleigh, D. P., Levitt, M. H., & Griffin, R. G. (1988) *Chem. Phys. Lett. 146*, 71.

Raleigh, D. P., Creuzet, F. J., Das Gupta, S. K., Levitt, M. H., & Griffin, R. G. (1989) *J. Am. Chem. Soc. 111*, 4502–4503.

Spiess, H. W. (1978) *NMR: Basic Prin. Prog. 15*, 59–207.

Spijker-Assink, M. B., Winkel, C., Baldwin, G. S., & Lugtenburg, J. (1988) *Recl. Trav. Chim. Pays-Bas 107*, 125.

Stam, C. H. (1972) *Acta Crystallog. B28*, 2936–2945.

Stam, C. H., & MacGillavry, C. H. (1963) *Acta Crystallogr. 16*, 62–68.

White, J. D., Skeean, R. W., & Trammell, G. L. (1985) *J. Org. Chem. 50*, 1939.

Wolff, E. K., Griffin, R. G., & Waugh, J. S. (1977) *J. Chem. Phys. 67*, 2387–2388.